IOP PUBLISHING NANOTECHNOLOGY

Nanotechnology **19** (2008) 225708 (5pp) doi:10.1088/0957-4484/19/22/225708

Molecular-beam epitaxy-grown Si whisker structures: morphological, optical and electrical properties

O V Naumova[1], Yu V Nastaushev[1], S N Svitasheva[1], L V Sokolov[1,2], N D Zakharov[2], P Werner[2], T A Gavrilova[1], F N Dultsev[1] and A L Aseev[1]

[1] Institute of Semiconductor Physics, SB RAS, 630090 Novosibirsk, Russia
[2] Max-Planck-Institut Für Mikrostrukturphysik, D-06120 Halle (Saale), Germany

E-mail: naumova@isp.nsc.ru

Received 16 January 2008, in final form 26 March 2008
Published 28 April 2008
Online at stacks.iop.org/Nano/19/225708

Abstract
Scanning electron microscopy, spectroscopic ellipsometry, and current–voltage and current–temperature measurements were employed to characterize nanowhisker structures grown by molecular-beam epitaxy on Si(111) substrates. Small clusters of gold deposited on the Si surface were used as the seeds for nanowhisker growth. The diameter of grown nanowhiskers and their length ranged from 70 to 200 nm and from 580 to 890 nm, respectively. The whiskers were found to inherit the (111) orientation of the Si substrate. By means of spectroscopic ellipsometry in the range 1.5–4.77 eV, lateral optical inhomogeneity of the nanowhisker layer was revealed, with optical properties of the layer substantially differing from those of single-crystal Si. Electrical measurements point to the presence of a Schottky barrier with height 0.70 eV in the structure and to the presence of electrically active centers non-uniformly distributed over the nanowhisker length.

1. Introduction

In recent years, silicon nanowhiskers (Si NWs), also called nanowires, nanopillars, or nanorods, have emerged as a subject of much research due to their interesting physical properties, and also due to the potential use of NW structures in novel nanoelectronic, optoelectronic and photovoltaic devices [1–5]. In particular, epitaxially grown Si NWs are presently considered as promising candidates for post-CMOS logic elements due to their potential compatibility with the well-established CMOS technology. The growth of vertical nanowires makes it possible to obtain vertical surround-gate field-effect transistors with better electrostatic gate control of the conducting channel, impossible in conventional planar architectures [4].

Various methods (chemical vapor deposition [6, 7], pulsed laser deposition [8], microwave plasma [9], molecular-beam epitaxy [10–14]) for Si NW growth have been reported lately and remarkable progress has been achieved in the fabrication of whiskers with predefined radius, length, and position on the substrate. Reproducibility of the structural and electrical properties of NWs is the key prerequisite for their application in various nanodevices; such reproducibility must therefore be ensured by NW fabrication methods.

The present study focuses on the properties of Si NW structures grown by molecular-beam epitaxy (MBE). The possibility to characterize such NW structures by means of spectroscopic ellipsometry and by electrical measurements using standard equipment and easily obtainable test samples has been examined. It was shown that such characterization may prove useful in monitoring the quality of grown NW structures and in optimization of NW fabrication processes.

Electrical measurements were performed on Si wafers with NWs covered with PMMA and aluminum layers. The thickness of the PMMA layer was varied so that electrical contact to whiskers of different length could be provided. The latter has allowed us to probe the physical properties of the NWs versus NW length.

We used also the non-destructive, non-disturbing method of the spectroscopic ellipsometry for quantitative evaluation of the nanowhisker structures. A clear correlation between optical spectra and whisker parameters is revealed.

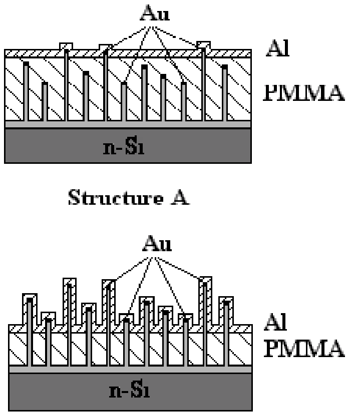

Figure 1. Schematic representation of structures A and B, used in electrical measurements, with electrical contact provided to 800–890 nm long NWs (structure A) and to all NWs (structure B).

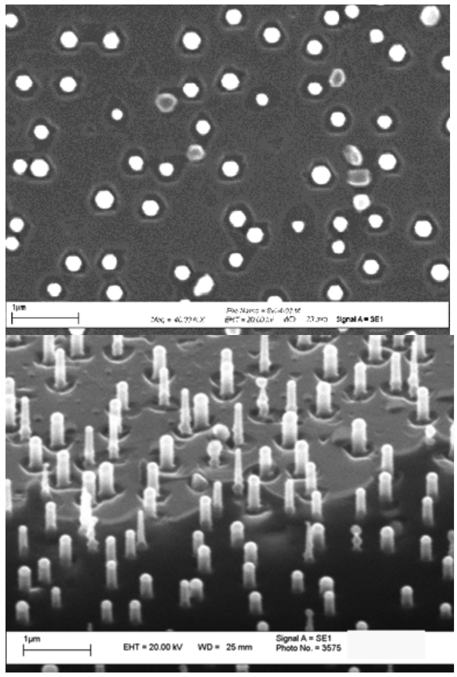

Figure 2. SEM images of grown NWs: top view (above) and tilt view (below).

2. Experimental details

Si NWs were grown by molecular-beam epitaxy. The substrates were (111)-oriented phosphorus-doped (5 Ω cm) Si wafers. Successive treatments, that included a cleaning procedure, deposition of a 100 nm thick Si buffer layer at 550 °C, deposition of a 2 nm thick Au layer at 520 °C, and growth of NWs at 520 °C, were carried out *in situ*, inside the MBE system (UHV chamber RIBER SIVA 45). A detailed description of the growth procedure is given elsewhere [12]. As a result, Si whiskers with hemispherical Au caps on their tops were fabricated. Each wafer with grown NWs was covered with a PMMA layer to avoid destruction of NWs during subsequent handling and to provide environmental control for the electrical measurements. The thickness of the PMMA layer was either 500 or 800 nm. Afterward, an Al layer was evaporated onto the PMMA layer to obtain electrical contact to the NWs. Two types of NW structure suitable for electrical measurements were prepared in this manner: structure A with electrical contact provided to the longest (800–890 nm) NWs, and structure B with electrical contact provided to the whole NW array (see figure 1).

Scanning electron microscopy (SEM), spectroscopic ellipsometry (SE), and current–voltage (I–V) and current–temperature (I–T) measurements were used to characterize the obtained NW structures.

I–T data were obtained for various bias voltages applied to the Al gate. In addition, mercury-probe tests were employed to examine the properties of the epitaxial Si (epi-Si) layer grown on the n-Si substrate by means of high-frequency capacitance–voltage (C–V) measurements.

3. Results and discussion

SEM images of the NW structures are shown in figure 2. The NWs are seen to protrude over the substrate normally to the substrate plane. Around each NW, there is a hollow that forms during the NW growth (detailed analysis of morphology of the MBE-grown Si whiskers including TEM has been published by authors in [12–14]).

Both the NWs and the hollows are faceted hexagonally, showing that the NWs have the same orientation as the Si(111) substrate. The length of the NWs was found to range from 580 to 890 nm; the average distance between them is from 720 to 850 nm; and the NW diameter is from 70 to 200 nm, thin NWs having larger lengths. The measured surface density of NWs varied depending on the measurement point on the wafer, as shown in table 1.

As is well known [15], spectroscopic ellipsometry deals with ellipsometric angles Ψ and Δ related to the relative reflection coefficient ρ by expression (1):

$$\tan\Psi e^{i\Delta} = \frac{R_p(E)}{R_s(E)} \equiv \rho(E), \quad (1)$$

where $R_p(E)$ and $R_s(E)$ are the Fresnel coefficients for p- and s-polarized light with photon energy E. In the general case of stratified planar structures, when R_p and R_s depend upon the parameters of all layers and the angle of light incidence ϕ_0, the ellipsometric spectra measured can be represented in terms of $\varepsilon_{pseudo}(E)$ if we disregard the actual structure of the sample, and accept it as semi-infinite homogeneous medium:

$$\varepsilon_{pseudo} = \langle\varepsilon_r\rangle + \langle\varepsilon_i\rangle = \tan^2\phi_o\left[1 + \frac{4\rho\sin^2\phi_o}{(1+\rho)^2}\right]. \quad (2)$$

Here, ε_r and ε_i are the real and imaginary parts of the pseudodielectric function, respectively.

The ellipsometric spectra of the complex pseudodielectric function measured at several points on the wafer with NWs are shown in figure 3. The NW layer is seen to be quite

Table 1. Volume fractions of thin NWs (diameters less than 130 nm) and thick NWs (diameters ranging from 130 to 200 nm), and the average distance between NWs at several measurement points on the substrate (points 1–3 in the inset to figure 3).

Position	Average separation between NWs (nm)	Volume fraction of all NWs (%)	Volume fraction of thin NWs (%)	Volume fraction of thick NWs (%)
1	740	7.8	2.2	5.6
2	850	6.0	1.4	4.6
3	725	7.8	3.3	4.5

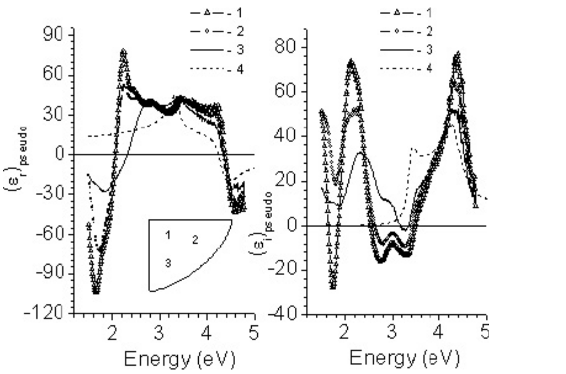

Figure 3. (1–3) ellipsometric spectra measured at points 1, 2, and 3, respectively (see the inset). These spectra are indicative of the lateral non-uniformity of the NW layer. The spectrum of c-Si (4) is given for comparison.

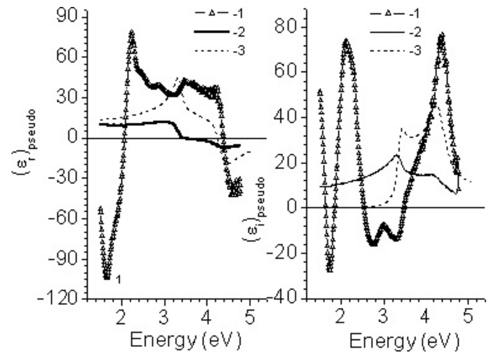

Figure 4. Ellipsometric spectra measured at one and the same point on the sample prior to (1) and after (2) the removal of Au caps from NWs by treating the sample in aqua regia. The spectrum of c-Si (3) is given for comparison.

transparent in the range of 1.5–2.6 eV; yet, the optical constants of the NW layer differ substantially from those of crystalline Si (c-Si), making it possible to observe the interference effect in the measured spectra. This effect depends on the measurement point on the structure as do the data in table 1. The absorption edge of the pseudodielectric function of NW structures is moved to considerably higher energies in comparison with c-Si. The number of transitions at 4.25 eV is seen to be greater than in the c-Si case. Generally, the spectra are dramatically distorted in the region with strong absorption (in the vicinity of the two critical points of Si: 3.43 and 4.25 eV).

In addition, the impact of semi-spherical Au-capped whiskers coupled with the decrease of NW heights is shown in figure 4, where the second spectrum corresponds to the first after removal of the Au caps by aqua regia. As a result of chemical treatment, the interband transitions at 3.43 and 4.25 eV are seen to decrease abruptly. Unfortunately, the chemical treatment clearly affected the whiskers, transforming them into stubs. As a result, the interference was found to disappear in the range of relative transparence of c-Si, although the optical properties of the NW layer still differed noticeably from those of c-Si. For the second spectrum it is possible to estimate the length of NWs as ∼20 nm, using the overlayer effective medium approximation (EMA) model with cylindrical islands and using scanning electron microscopy (SEM) data from table 1. The SEM image of this sample confirmed our calculation.

It was revealed that the whiskers inherit the Si crystal orientation but their composition is non-constant along the whisker [12, 14], and includes oxidized and eutectic layers. In our opinion, it will be necessary to consider in detail such effects as geometrical shadow, formation of oxide and eutectic layers, refraction by transparent whisker bodies and reflection of Au caps. It is necessary to notice that the creation of an optical model for whiskers is a very difficult task which is waiting solution. However, to explain these effects observed in the spectra by means of calculation, the dielectric function of just the NWs layer should be described by some model and then the parameters of model will be obtained from measured spectra. The effective medium approximation (EMA) based on the theory of additivity for a mixture of several components (in volume fractions) is used as a rule to describe the dielectric function of a non-homogeneous layer. Figure 2 and table 1 show, on the one hand, a large length of NWs in the layer ($L \gg \lambda$), and on the other hand, their small volume fraction. Unfortunately, under these conditions EMA is not available for modeling a layer similar to the NW layer.

The ellipsometric spectra of NW structures in the range 1.5–4.77 eV differ from those of c-Si, making it possible to inspect such structures for planar uniformity and to check the reproducibility of NW structures grown by various methods because the height and distribution of whiskers over the substrate impact on measured spectra noticeably. Thus immediately after the recording of the spectra, SE can be profitably employed as non-destructive, non-disturbing technique without modeling and any calculations (problems of optical modeling of NW structures are not solved yet for NWs with length about 1 mm (as shown in figure 1) and with variable composition (as shown earlier in [12, 14, 16]) along the whisker).

Current–voltage characteristics measured on structures A and B are shown in figure 5. The I–V curve measured on the epi-Si/substrate stack (structure without NWs) is also

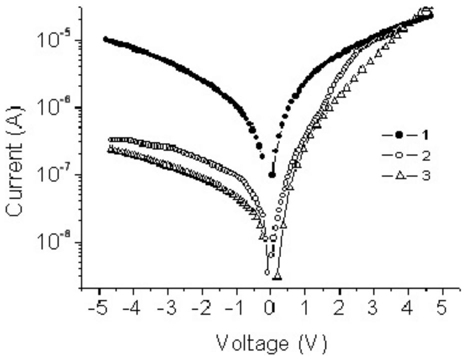

Figure 5. Current–voltage characteristics of the epi-Si/substrate stack (1), structure B (2), and structure A (3). The positive bias applied to the NWs (or to the epitaxial Si layer) is in the forward direction and the negative bias is in the reverse direction.

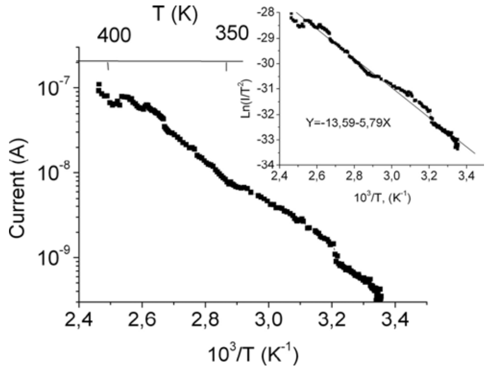

Figure 6. The electric current through structure A under bias voltage $V_F = 0.2$ V versus the reciprocal temperature. The inset shows a linear fit of $\ln(I/T)$ versus $1/T$.

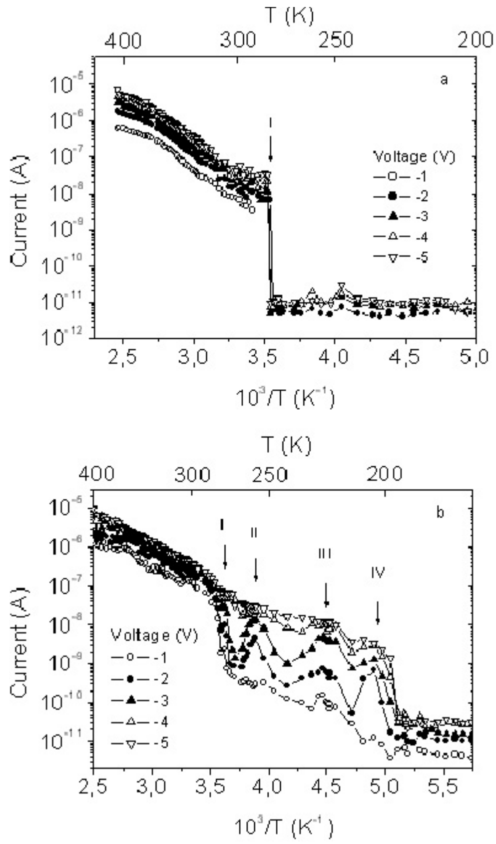

Figure 7. The electric currents through structures A and B ((a) and (b), respectively) measured at different reverse biases versus the reciprocal temperature.

shown for comparison. The NW structures displayed a well-pronounced rectifying behavior, with the current ratio I_F/I_R amounting to $\sim 10^2$ at $V_g = 5$ V. Almost no rectifying effect was observed in the structure without NWs, making us conclude that the rectifying property of the NW structures was due to the Schottky barrier formed between the metal contact and the NWs rather than due to the barrier between the epi-Si layer and the substrate.

The forward current (at $V = 0.2$ V) through structure A versus temperature is shown in figure 6. The height of the Schottky barrier making the current–voltage characteristics of the structure asymmetric was estimated from the plot of $\ln(I/T^2)$ versus $1/T$ [17]. This height turned out to equal 0.70 eV.

The currents through structures A and B measured versus temperature at different reverse biases V are shown in figure 7. The curves for structure A display the following interesting features: the current through structure A (1) exponentially decreases with the temperature in the interval from 400 to 280 K, (2) abruptly falls in value at $T_I = 280$ K, and (3) weakly depends on temperature at temperatures $T < 280$ K. The current through structure A as a function of temperature behaves similarly at other bias voltages. Unlike in structure A, the current through structure B is almost independent of temperature at $T < 200$ K, yet at higher temperatures ($T > 200$ K) it depends on the bias voltage applied to the structure. The current through structure B (1) also abruptly decreases at $T_I = 280$ K with decreasing temperature, this effect being observed only at reverse biases $V = (1–3)$ V; (2) non-monotonically decreases with temperature within the temperature range 280–200 K at the reverse biases 2 and 3 V, displaying peaks at $T_{II} = 257$ K and $T_{III} = 224$; and (3) abruptly decreases at $T_{IV} \sim 200$ K for bias voltages $V = (2–4)$ V.

These observations allow us to conclude that (1) the conduction through structures A and B at $T < 280$ K is the conduction through NWs and (2) NWs contain at least four different types of recharging center (centers I–IV) non-uniformly distributed over the whisker length and manifesting themselves in the peaks displayed by the I–T curves at temperatures below 280 K.

The position of centers I–IV over the NW length can be evaluated using the expression for the width of the depletion region in a Schottky contact [17]:

$$W(V) = \sqrt{\frac{2\varepsilon(\varphi_c - V)}{qN}}. \quad (3)$$

Here, ε is the dielectric permittivity, φ_c is the built-in potential, V_g is the reverse bias applied to the structure (at which peaks

Table 2. Regions over whisker length in which centers I–IV are localized in the NWs.

Center	$W_{max} - W_{min}$ (nm)
I	890–264
II	528–264
III	5280–264
IV	Below 528

due to centers I–IV are observed), q is the electron charge, and N is the doping concentration.

Centers I were observed in structure A at reverse biases $V = (1–5)$ V and in structure B at $V = (1–3)$ V (figure 7). The maximum and minimum NW lengths were found to equal 890 and 580 nm, respectively. Thus, centers I are located along the NWs in the region from $W_{max} = 890$ nm to $W_{min} = 580 - W(3\text{ V})$. The estimate of W_{min} yields $W_{min} = 264$ nm on the assumption that the doping concentration in NWs coincides with the doping concentration N found from the C–V measurements of the epi-Si layer/substrate stack (about 5×10^{16} cm^{-3}). The position of all other centers in the NWs was determined in a similar way. The regions over whisker length in which centers I–IV are localized are summarized in table 2.

As for the origin of the centers observed, it can be speculated that the thermally stimulated currents observed at the temperatures T_{II}, T_{III}, and T_{IV} (see figure 7) may be due to Au atoms with the acceptor level $E_c - 0.55$ eV in the Si bandgap [18] and/or due to dislocations, which were revealed in MBE-grown NWs in [12]. Dislocations have deep levels whose energy position was estimated as $E_c - 0.22$ eV, $E_c - 0.31$ eV, $E_c - 0.41$ eV, and $E_c - 0.58$ eV [19]. It is interesting that one of the energy levels due to oxygen-related thermal donors in the bandgap of Si lies at $E_c - 0.15$ eV [18], which value coincides closely with the position of the Fermi level in the NWs at the temperature T_I. The freeze-out of the NW conductivity at $T_I = 280$ K seems to be due to change in the charge state of donor complexes (contaminations, defects).

4. Conclusion

Si NWs can be characterized by electrical measurements using easily obtainable test structures prepared by covering the NW layer with a PMMA film of variable thickness and, then, depositing onto the PMMA film a contact Al layer.

The MBE-grown Si NWs with Au drops on top, studied by means of scanning electron microscopy, spectroscopic ellipsometry, and current–voltage and current–temperature measurements, were found to have the following characteristics. The diameter of the NWs was in the range 70–200 nm, the length of the NWs was in the range 580–890 nm, and the average separation between the NWs varied from 720 to 850 nm.

A Schottky barrier with height 0.70 eV is the cause for rectification in the examined structures and for the exponential behavior of the I–T curves in the temperature interval 400–280 K.

The NWs contain electrically active centers non-uniformly distributed over the NW length. These centers can be tentatively identified as oxygen-related thermal donors, dislocations, and/or Au atoms. Changes in the charge state of these centers are responsible for the observed freeze-out of NW conductivity at $T = 280$ K and for the thermally stimulated currents observed in the NW structures at temperatures below 280 K.

Ellipsometric spectra of NW structures in the range 1.5–4.77 eV differ from those of c-Si, making it possible to inspect such structures for planar uniformity and check the various fabrication methods for NW structures for reproducibility. Ellipsometry proved to be a very attractive (non-destructive, non-disturbing) tool, permitting investigation of such delicate and complicated objects as NW structures and getting a quantitative evaluation of their parameters.

A clear correlation between the optical spectra and the whisker parameters is revealed. Problems of optical modeling of NW structures have been solved now for NWs with length less 25 nm; the problem of optical modeling is not solved for NWs with length about 1 mm and with variable composition along the whisker.

Acknowledgments

This work was supported in part by the Russian Foundation for Basic Research (Grants Nos 04-02-16541 and 04-02-16747).

References

[1] Pooley D M, Ahmed H, Mizuta H and Nakazato K 1999 *Appl. Phys. Lett.* **74** 2191
[2] Scheible D V and Blick R H 2004 *Appl. Phys. Lett.* **84** 4632
[3] Tilke A, Blick R H, Lorenz H and Kotthaus J P 2001 *J. Appl. Phys.* **89** 8159
[4] Smiidt V, Riel H, Senz S, Karg S, Riess W and Gosele U 2006 *Small* **2** 85
[5] Peng K, Xu Y, Wu Y, Yan Y, Lee S-T and Zhu J 2005 *Small* **1** 1062
[6] Kamins T I, Williams R C, Hesjedal T and Harris J S 2002 *Physica* E **13** 995
[7] Wu Y, Fan R and Yang P 2002 *Nano Lett.* **2** 83
[8] Morales A M and Liber C M 1998 *Science* **279** 208
[9] Sunkara M K, Sharma S, Miranda R, Lian G and Dickey E C 2001 *Appl. Phys. Lett.* **79** 1546
[10] Liu J L, Cai G L, Jin S G, Thomas S G and Wang K L 1999 *J. Cryst. Growth* **200** 106
[11] Zhang Y, Zhang Q, Wang N, Yan Y, Zhou H and Zhu J 2001 *J. Cryst. Growth* **201** 185
[12] Schubert L, Werner P, Zakharov N D, Gerth G, Kolb F M, Long L and Gösele U 2004 *Appl. Phys. Lett.* **84** 4968
[13] Zakharov N D, Werner P, Gerth G, Schubert L, Sokolov L and Gosele U 2006 *J. Cryst. Growth* **290** 6
[14] Zakharov N, Werner P, Sokolov L and Gosele U 2007 *Physics* E*: Low-dim. Sys. Nano.* **37** 148
[15] Azzam R M A and Bashara N M 1977 *Ellipsometry and Polarized Light* (Amsterdam: North-Holland)
[16] Svitasheva S N, Sokolov L V, Zakharov N D and Werner P 2007 *Proc. ICSE-4 (Stockholm)* p 290
[17] Szi S M 1981 *Physics of Semiconductor Devices* (New York: Wiley)
[18] Bridgest F, Devies G, Robertson J and Stoneham A 1990 *J. Phys.: Condens. Matter* **2** 2875
[19] Kimerling L C 1988 *Point and Extended Defects in Semiconductors: Proc. NATO Advanced Research Group* (*NATO Advanced Study Institute Series* vol 202) ed G Benedek, A Cavallini and W Schroter (New York: Plenum)